

Cold Atom Ion Sources

J. J. McClelland,¹ J. R. Gardner,¹ W. R. McGehee,¹ A. Schwarzkopf,² B. Knuffman,² and A. V. Steele²

¹*Alternative Computing Group, National Institute of Standards and Technology, Gaithersburg, Maryland 20899 USA*

²*zeroK NanoTech Corporation, Gaithersburg, MD 20779 USA*
jabez.mcclelland@nist.gov

Ionization of laser-cooled atoms has emerged as a new approach to constructing high brightness ion sources for applications such as focused ion beam (FIB) microscopy and milling. While conventional sources, such as the Ga liquid metal ion source (LMIS) or the gas field ionization source (GFIS), attain brightness by emitting from a very sharp tip, cold atom sources reach high brightness through reducing the transverse velocity spread of the ions. With the ultracold, microkelvin-range temperatures achievable with laser cooling, the corresponding velocity spread can lead to a brightness significantly higher than typical LMIS values. Moreover, the phase-space shape of the emittance of the source – narrow in velocity, wide in space – brings new opportunities for ion optical design. For example, high currents can be obtained without the high current density present in sharp tip sources. This can result in reduced Coulomb effects, such as increased emittance and broadened energy spread (Boersch effect). In addition, the absence of a sharp tip can reduce sensitivity to source stability. Other advantages of this type of source include insensitivity to contamination, access to new ionic species, inherent isotopic purity, and fine control over emission, down to the single ion level. To date, sources have been demonstrated with Cr,¹ Li,² Rb,³ and Cs^{4,5} ions, realizing novel species and nanometer-scale spot sizes. In this talk I will review progress in the field and discuss recent developments in Li ion sources and applications.

¹A.V. Steele, B. Knuffman, J.J. McClelland, and J. Orloff, *J. Vac. Sci. Technol. B* **28**, C6F1 (2010).

²B. Knuffman, A.V. Steele, J. Orloff, and J.J. McClelland, *New J. Phys.* **13**, 103035 (2011).

³G. ten Haaf, T.C.H. de Raadt, G.P. Offermans, J.F.M. van Rens, P.H.A. Mutsaers, E.J.D. Vredembregt, and S.H.W. Wouters, *Phys. Rev. Applied* **7**, 054013 (2017).

⁴A.V. Steele, A. Schwarzkopf, J.J. McClelland, and B. Knuffman, *Nano Futures* **1**, 015005 (2017).

⁵M. Viteau, M. Reveillard, L. Kime, B. Rasser, P. Sudraud, Y. Bruneau, G. Khalili, P. Pillet, D. Comparat, I. Guerri, A. Fioretti, D. Ciampini, M. Allegrini, and F. Fuso, *Ultramicroscopy* **164**, 70 (2016).

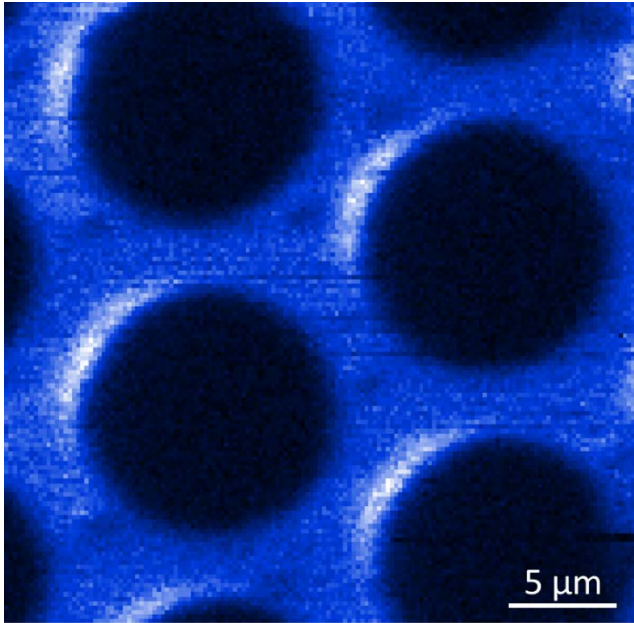


Fig 1. Secondary electron image of a microchannel plate obtained with a Cr FIB [from ref. 1].

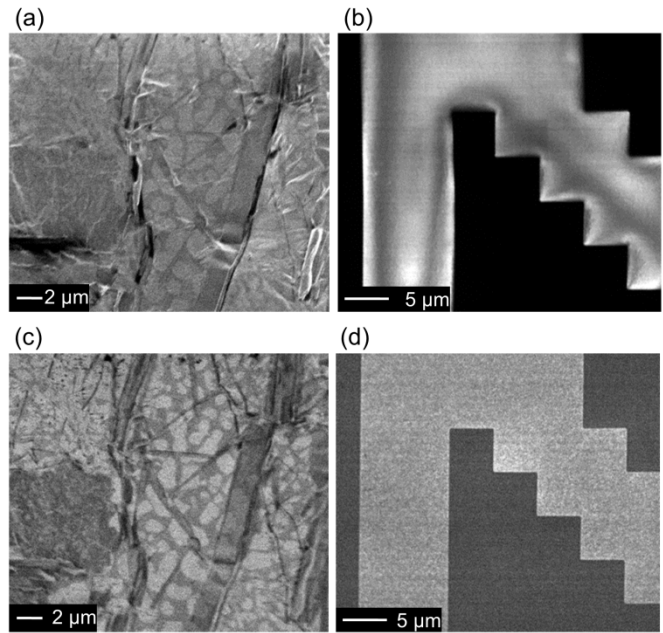


Fig 2. Lithium ion microscope images. (a) Secondary electron and (c) backscattered ion images of a lead-tin solder dot. (b) Secondary electron and (d) backscattered ion images of a metal on oxide test pattern. [from K. A Twedt *et al.*, *Ultramicroscopy* **142**, 24 (2014)].

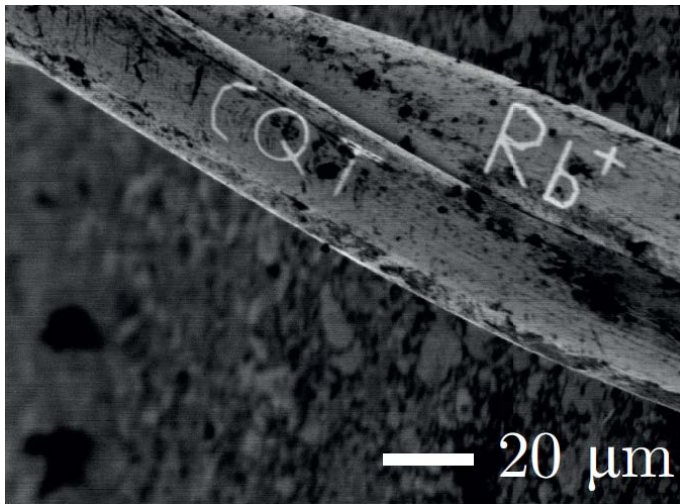


Fig 3. Secondary electron image of bond wires obtained with a Rb FIB, showing milled writing [from G. ten Haaf, PhD thesis, Technische Universiteit Eindhoven (2017)].

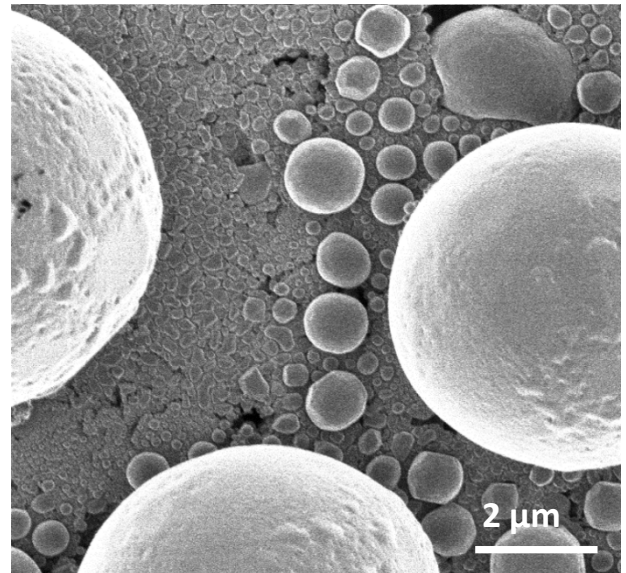


Fig. 4 Secondary electron image of a tin ball resolution target obtained with a Cs FIB [from ref. 4].